ionization, step ionization, three-particle recombination, dissociative recombination, and radiative recombination, respectively; n_*) concentration of excited atoms; I) ionization potential; σ_0) effective cross section of ionization by electron impact; i) ionic current at the probe; m_g) mass flow rate of plasma-forming gas; P) pressure in plasma jet; e) elementary charge; m) mass of argon molecule; S) distance from nozzle cross section of plasmotron; l) plate thickness; τ) time of plate burnthrough.

LITERATURE CITED

1. A. Khasui, Sputtering Techniques [in Russian], Moscow (1975).
2. D. A. Rodchenko, M. I. Petrokovets, and A. I. Barkan, Vestsi Akad. Nauk B. SSR, Ser. Fiz.-Tekh. Navuk, No. 4, 52-56 (1983).
3. V. V. Kharitonov and O. R. Yurkevich, Inzh.-fiz. Zh., 50, No. 3, 379-385 (1986).
4. Yu. V. Polezhaev and F. B. Yurevich, Thermal Shielding [in Russian], Moscow (1976).
5. Yu. P. Raizer, Usp. Fiz. Nauk, 99, 687-728 (1969).
6. L. A. Sena, Physics Dictionary [in Russian], Moscow (1983), p. 654.
7. V. D. Rusanov, and A. A. Fridman, Physical Chemistry of Active Plasma [in Russian], Moscow (1984).
8. A. V. Donskoi, V. S. Klubnikin, and A. A. Salangin, Zh. Tekh. Fiz., 55, No. 11, 2124-2128 (1985).
9. S. F. Zhandarov, A. Z. Skorokhod, and O. R. Yurkevich, Vesti Akad. Nauk B. SSR, Ser. Fiz.-Tekh. Navuk, No. 1, 39-43 (1990).
10. V. A. Belyi, V. A. Dovgyalo, and O. R. Yurkevich, Polymer Coatings [in Russian], Minsk (1976).
11. S. Madorskii, Thermal Decomposition of Organic Polymers [in Russian], Moscow (1967).

CALCULATION OF THE DRYING OF MOIST PARTICLES IN APPARATUS CONTAINING OPPOSED SWIRLED STREAMS

I. Kh. Enikeev

UDC 582.5:533.6.011

A method is suggested that enables one, in the model of interpenetrating continua, to investigate heat and mass transfer between a gas and moist particles in swirled streams. Similarity criteria are obtained for modeling an extensive class of problems of chemical engineering.

Swirled flows of multiphase media are used extensively in modern technology (chemical engineering apparatus, turbomachines, cryogenics, etc.) to intensify processes of heat and mass transfer and separation. Two types of heterogeneous media are used most often in industrial devices: 1) gas–drop and vapor–drop streams; 2) gas suspensions (a gas containing dessicant or moist solid particles in a suspended state).

Whereas the theory for the first class of flows and methods of calculating heat and mass transfer have been presented fairly completely in [1-3], for a gas containing moist solid particles in a suspended state, models of heat and mass transfer have been developed only for the case of a low mass content of the disperse phase. The approaches developed in [4-6] to investiate the theory of heat and mass transfer between moist solid particles and a gas stream (drying theory) do not enable one to model and calculate the drying process for a high content of the disperse phase, when the influence of the particles on the motion of the carrier gas must be taken into account. In the present paper, therefore, it is proposed to investigate the drying process in a model of interpenetrating continua, enabling us to model that process in a wide range of variation of the mass concentration of particles.

Moscow Institute of Chemical Mechanical Engineering.

Translated from Inzhenerno-fizicheskii Zhurnal, Vol. 61, No. 5, pp. 770-777, November, 1991. Original article submitted February 27, 1991.

0022-0841/91/6105-1361$12.50

In the present paper, on the basis of the model of interpenetrating continua, we investigate the process of drying of a disperse material in an apparatus with opposed swirled streams. We show that such apparatus is efficient not only for cleaning a disperse impurity from industrial wastes but also for drying most products in various branches of industry.

Mass transfer between phases is estimated for both low and high mass concentrations of particles in the disperse stream.

Statement of the Problem

The numerous methods of investigating the drying process, developed in [4-6] and others, describe that process fairly completely in various drying apparatus of the rotary drum type, with a fluidized bed, cyclone and spiral apparatus, etc. Nevertheless, the use of those methods and of the corresponding dryers is limited by a number of conditions, one of which is that the mass concentration of moist particles in the disperse stream is $r_{20} \ll 1$. This condition enables one to assume that the motion of the single particles occurs in the given velocity field of the carrier gas, which considerably simplifies the problem. Many of today's dryers, however, including apparatus with opposed swirled streams (AOSS), operate in a regime in which the content of the moist product in the gas suspension at the entrance section of the dryer is fairly high, $r_{20} \simeq 1$. For the optimum design of a production line including a dryer in this case, one must allow for the influence of the particles on the hydrodynamic parameters of the gas.

Let us consider the schematic diagram of operation of an apparatus with opposed swirled streams. As shown in Fig. 1, an AOSS consists of a vertical cylindrical housing, to the lower part of which the disperse stream, called the primary stream below, is supplied through a supply pipe 1 coaxially with a swirler 5 of the axial-vane or helical type. A cowling 6 is located in the central part of the swirler 5. A deflecting disk 9, separating the AOSS housing from the hopper 10, is located on the outside of the swirler. The diameter of the deflecting disk 9 is 0.95D (D is the diameter of the cylindrical part of the housing 4), providing an annular slit for transport of the disperse product into the hopper. In the upper part of the housing of the apparatus is a swirler 3, to which the secondary dusty stream is supplied tangentially through the supply channel of the collector 2 in an amount G_2. The quantities G_1 and G_2 of the primary and secondary disperse streams are determined by the through cross sectional areas of the swirlers 5 and 3, as well as by the flow rate G in the apparatus 7. Thus, the interaction of disperse streams swirled in the same direction occurs in the cylindrical part 4 of the apparatus. The stream interaction is organized so that the secondary stream travels to the deflecting disk 9, turns around, and together with the primary stream travels toward the outlet pipe 8. Centrifugal force throws particles of the moist product out toward the side wall of the apparatus, where they are carried by the secondary stream through the annular slit 11 into the hopper 10. The stream from which the solid phase has been cleaned is extracted from the apparatus through the outlet pipe 8. A schematic diagram of the stream interaction in the longitudinal plane of an apparatus that reflects the above-described AOSS construction is shown in Fig. 2. We assume that the particle

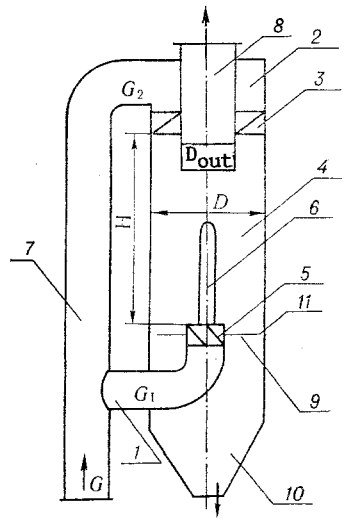

Fig. 1. Schematic diagram of an apparatus with opposed swirled streams.

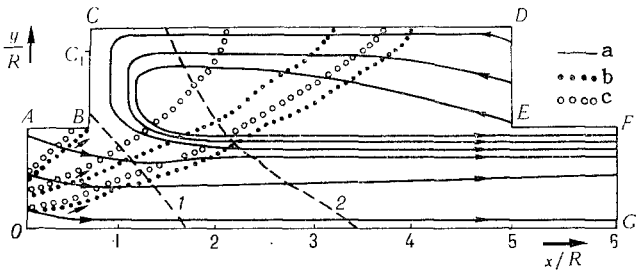

Fig. 2. Streamlines of gas and particles: a) gas; b) particles, $\alpha_{l0} = 0.3$; c) particles, $\alpha_{l0} = 0.8$. Curves 1 and 2 correspond to $\alpha_{l0} = 0.3$ and 0.8.

size does not change during drying. As in [4], we assume that the moisture is distributed uniformly over the entire volume of a particle. The true mean density of a particle is then

$$\rho_2^0 = \alpha_p \rho_p^0 + \alpha_l \rho_l^0,$$

where $\rho_p{}^0$ and $\rho_l{}^0$ are the true densities of the material and water, and α_p and α_l are the volume content of the material and water in a moist particle ($\alpha_p + \alpha_{l0} = 1$); α_{l0} is the relative moisture content of a particle in the entrance cross section OA. Following [1], we assume that phase transitions at the surface of a moist particle occur by means of evaporation and stripping. Moisture is evaporated from a particle due to the heat flux from the gas to the particles. Here we assume that all of the heat supplied to a moist particle goes into overcoming the binding between the particle and moisture (the binding energy being directly proportional to the specific heat of vaporization l, as shown in [4]) and into heating and evaporating the liquid. Such a model of evaporation from the surface of a moist particle is called the theoretical drying regime [5]. Stripping of the surface layer from a moist particle occurs by the separation of fine drops with their subsequent instantaneous evaporation in the gas stream (cold drying regime). The internal structure of a particle, as well as such processes as liquid filtration through its pores, diffusion of liquid molecules from the surface of the moist particle into the gas stream, the formation of a vapor envelope around the particle, etc., were not taken into account in the investigation of drying. We also assumed a uniform temperature profile inside a particle; the velocities and thermophysical properties of the gas, separated small drops, and vapor coincide; coagulation and breakup of particles are absent.

Equations of Motion

In the proposed model, the initial equations have the form [1]

$$\frac{\partial \rho_i}{\partial t} + \operatorname{div}(\rho_i \mathbf{v}_i) = (-1)^{i-1} n [j^{(S)} + j^{(T)}], \quad \frac{\partial n}{\partial t} + \operatorname{div}(n\mathbf{v}_2) = 0,$$

$$\frac{\partial \rho_i \mathbf{v}_i}{\partial t} + \nabla^k (\rho_i v_l^k \mathbf{v}_i) + (2-i)\nabla p = (-1)^i n \mathbf{f}_{12} + (-1)^{i-1} n [j^{(S)} + j^{(T)}] \mathbf{v}_2, \tag{1}$$

$$\frac{\partial}{\partial t}\{\rho_1 E_1 + \rho_2 E_2\} + \operatorname{div}(\rho_1 E_1 \mathbf{v}_1 + \rho_2 E_2 \mathbf{v}_2 + p\mathbf{v}_1) = 0,$$

$$(E_i = e_i + 1/2 v_i^2), \frac{\partial \rho_2 e_2}{\partial t} + \operatorname{div}(\rho_2 e_2 \mathbf{v}_2) = n q_{12} - n [j^{(S)} + j^{(T)}] e_2.$$

The system (1) is closed by the equations of state of the phases,

$$p = \rho_1^0 R_1 T_1, \; u_1 = c_{v1}(T_1 - T_2) + u_{10},$$

$$i_1 = c_{p1}(T_1 - T_{10}) + i_{10}, \; u_2 \approx c_2 (T_2 - T_{10}) + u_{20},$$

$$i_2 \cong c_2 (T_2 - T_{10}) + i_{20}, \; i_{10} - i_{20} = l + (c_2 - c_{p1})(T_S - T_{10}),$$

$$c_2 = \frac{c_p \alpha_p + c_l \alpha_l}{\alpha_p + \alpha_l}, \; \rho_p^0 = \text{const}, \; \rho_l^0 = \text{const}.$$

The expressions for the force interaction and thermal interaction between the phases have the form

$$\mathbf{f}_{12} = \frac{\pi d^2}{8}\rho_1^0 C_d |\mathbf{v}_1 - \mathbf{v}_2|(\mathbf{v}_1 - \mathbf{v}_2),$$

$$C_d = \frac{24}{\mathrm{Re}_{12}} + \frac{3}{\sqrt{\mathrm{Re}_{12}}} + 0{,}4, \tag{2}$$

$$q_{12} = \pi d\lambda_1 \mathrm{Nu}(T_1 - T_2),\ \mathrm{Nu}_{12} = 2 + 0{,}6\,\mathrm{Re}_{12}^{1/2}\mathrm{Pr}^{1/3},\ \mathrm{Pr} = \frac{c_{p1}\mu_1}{\lambda_1}.$$

By analogy with [2], we specify the intensities of stripping $j^{(S)}$ and evaporation $j^{(T)}$ as follows:

$$j^{(S)} = \begin{cases} j_*^{(S)}, & \mathrm{We}_{12} \geqslant \mathrm{We}_c, \\ 0, & \mathrm{We}_{12} < \mathrm{We}_c, \end{cases}$$

$$\mathrm{We}_c = 0{,}5\sqrt{\mathrm{Re}_c},\ j_*^{(S)} = k^{(J)}(\rho_1^0)^{1/6}(d/2)^{3/2}|\mathbf{v}_1 - \mathbf{v}_2|, \tag{3}$$

$$k^{(J)} \cong 1{,}3 - 2\,\frac{\mathrm{kg}^{5/6}}{\mathrm{m}^{3/2}\cdot\mathrm{sec}^{1/2}},\ \mathrm{We}_{12} = \frac{\rho_1^0 d|\mathbf{v}_1 - \mathbf{v}_2|^2}{\sigma},$$

$$j^{(T)} = \begin{cases} j_*^{(T)}, & j^{(S)} = 0 \text{ and } T_2 = T_s, \\ 0, & j^{(S)} \neq 0 \text{ or } T_2 < T_s, \end{cases}$$

$$j^{(T)} = \frac{q_{12} - \varkappa l}{l},\ \varkappa \sim \frac{q_{12}}{2l},\ T_s = \frac{T_*}{p_* - \ln p}. \tag{4}$$

Equations (3) were written with allowance for the assumption that no evaporation occurs during stripping of the surface layer, since it has been shown [1] that during stripping the heat flux cannot penetrate through the stripped layer of liquid, so no heat transfer occurs between the gas and the liquid inside the particle.

The initial system of equations (1) and the closing equations (2)-(4) were normalized to the parameters of the gas in the undisturbed stream. For the characteristic scales of length and time we used R and $\tau = R/U_0$. As a result of the normalization, we obtain the following main similarity criteria:

$$M_0,\ r_{20} = \frac{\rho_{20}}{\rho_1^0},\ \alpha_p,\ \alpha_{l0},\ \beta^{(v)} = \frac{8\rho_{20}^0 d}{3\rho_1^0 R},$$

$$\mathrm{Re}_d = \frac{\rho_1^0 U_0 d}{\mu_1},\ \beta^{(\tau)} = \frac{\rho_{20}^0 d^2 U_0 c_{20}}{3{,}6\,\lambda_1 R\sqrt{\mathrm{Re}_d}\,\mathrm{Pr}^{1/3}}.$$

$$\left(\beta^{(\tau)} = \beta^{(v)}\frac{\sqrt{\mathrm{Re}_d}\,c_{20}}{10\,\gamma c_{v1}}\mathrm{Pr}^{1/3} \text{ for } \mathrm{Re}_{12} \gg 1\right),$$

$$j_0^{(S)} = \frac{U_0^{1/2} d^{3/2}\rho_{20}^0}{(\rho_1^0)^{1/6} R},\ j_0^{(T)} = \frac{c_{v1} l \rho_{20}^0 d^2}{6R\lambda_1 U_0}, \tag{5}$$

$$\beta^{(\tau)} \simeq \frac{c_2}{c_{v1}}\frac{U_0^2}{l}\frac{1}{\mathrm{Pr}^{2/3}\mathrm{Re}_d^{1/2}},\ \mathrm{We}_d = \frac{\rho_1^0 d U_0^2}{\sigma},\ \frac{T_{10}}{T_{20}},\ \gamma,\ \frac{c_{v1}}{c_p}, \tag{6}$$

and c_ℓ/c_p, as well as the kinematic and geometrical parameters characterizing the gas stream and the region under consideration.

The following problem was analyzed within the framework of the proposed model. A two-phase medium, consisting of a carrier gas and monodisperse moist particles, moves in a cylindrical channel of radius R and length L (L > 2R). A sketch of half of the longitudinal cross section of the channel, schematically depicting the modern construction of a non-entraining dryer, is shown in Fig. 2. The line OG is the axis of symmetry; the primary two-phase stream is supplied by means of swirlers through the cross section OA. The stream emerges freely from the apparatus through the cross section FG. The annular cross section DE serves to introduce the opposite stream, which is swirled in the same direction as the primary stream, into the apparatus. The counterstream helps to remove from the apparatus,

through the annular slit CC_1, particles collected near the wall CD under the action of centrifugal force. The end-type entry of gas and moist particles, distributed uniformly over the channel cross section, enables us to treat the flow of the two-phase medium in the channel as axisymmetric. The initial and boundary conditions for the system (1) in the region shown in Fig. 1 were set up by analogy with what was done in [7].

Scheme of Numerical Integration and Results

The problem formulated above was solved numerically by a modified method of large particles [7]. The modification consisted in the use of a difference scheme, implicit with respect to time, in the Euler stage, enabling us to carry out calculations for fairly low Mach numbers M_0 ($M_0 \lesssim 0.1$) typical of most chemical engineering problems. A scheme of first-order precision was used. The precision was monitored by comparing numerical solutions obtained on grids with different numbers of cells and with different time step sizes. The difference between the results of all the versions did not exceed 3-5%. To test the adequacy of the proposed model to the physics of the process under consideration, we compared the calculated results with certain experimental data given in [4, 5]. The difference between the drying curve for a disperse material obtained in calculations based on the suggested model and the corresponding experimental curve obtained in [4, 5], in particular, is several percent. Just as in the ordinary method of large particles [8], in the Euler stage intermediate values are calculated only for the gas phase. The parameters of the disperse phase remain constant in this stage, since the pressure gradient does not appear in the equations for the solid phase. The transfer of mass, momentum, and energy of each phase through the cell boundaries is calculated in the Lagrange stage. In the concluding stage, the values of the parameters of all of the phases in the new time layer are found on the basis of the laws of conservation of mass, momentum and energy. Here the force interaction (f_{12}), thermal interaction (q_{12}), and interphase mass transfer ($j^{(S)}$ and $j^{(T)}$) are taken into account. As in the usual scheme of the method of large particles [8], the parameters of the solid phase are first calculated algorithmically. In the main versions, the length of the calculation region, shown in Fig. 2, was divided into 74 intervals and the radius into 14 intervals. The dimensionless integration step size in space Δx was taken to be 1/12. The dimensionless integration step size in time $\Delta\tau$ was determined from the condition $\Delta\tau/\Delta x = 0.1$. The calculations were carried out for different values of the dimensionless determining parameters and geometrical dimensions of the region.

An analysis of the drying mechanism showed that for small $\beta^{(v)}$ ($\beta^{(v)} \leq 0.5$), we have $We_{12} < We_c$, so phase transitions occur only due to evaporation of moisture contained in the particles. With increasing $\beta^{(v)}$, the heat flux q_{12} per unit phase interface decreases for a given r_{20} [from (5) it follows that $\beta^{(\tau)} \propto \beta^{(v)}$, while $q_{12} \propto 1/\beta^{(v)}$], while the inertia of the particles increases, owing to which We_{12} increases and, starting with a certain $\beta^{(v)}$ ($\beta^{(v)} \approx 40$), $We_{12} > We_c$. Particle drying then occurs only due to the stripping of small drops from the surface of a moist particle and the instantaneous evaporation of those drops in the gas stream. It is thus quite obvious that a range of $\beta^{(v)}$ exists in which $We_{12} < We_c$, while $\beta^{(\tau)}$ is so large that moisture evaporates very slowly from the particle surface [from (6) it follows that $j_0^{(T)} \propto \beta^{(v)}$ and $j^{(T)} \propto 1/j_0^{(T)}$]. Calculations to determine this range of $\beta^{(v)}$ showed that for differentials between gas and particle temperatures $T_{10}/T_{20} = 1.5$-5 in cross section OA, the initial moisture content α_{10} of the particles changes insignificantly for $\beta^{(v)} \approx 4$. For $T_{10}/T_{20} = 2$, for example, the maximum decrease from the initial moisture content in the particles is 1%, while for $T_{10}/T_{20} = 5$ it is 17%. In an investigation of the stripping process it is important to know the influence of α_{10} on the stream hydrodynamics in the region under consideration.

In Fig. 2 we give streamlines of the carrier phase and particle streamlines in an axisymmetric channel in the presence of opposed swirled streams. Here a dashed curve denotes the boundary between the region in which drying of the disperse particles occurs and the region in which it does not. The results given in Fig. 2 were obtained for the following values of the dimensionless determining parameters: $M_0 = 0.08$; $r_{20} = 1$; $\beta^{(v)} = 44$; $k_\omega^{OA} = k_\omega^{DE} = 3.6$; $U_{DE} = -0.5$; $T_{10}/T_{20} = 2$; $j_0^{(S)} = 0.03$; $j_0^{(T)} = 62 \cdot 10^5$; $We_d = 7$; $Re_d = 1082$.

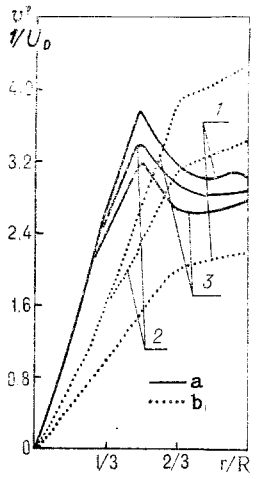

Fig. 3. Distributions of the tangential component of gas and particle velocities over a cross section of the apparatus: a) gas; b) particles; 1) α_{l0} = 0.3; 2) 0.6; 3) 0.8.

In the calculations we assumed that in the cross sections OA and ED the gas is swirled as a solid body ($v_1^{\varphi} \propto r$), the axial velocity components are distributed uniformly over the entrance cross sections, and the radial velocity components vanish. We also assumed no velocity slippage between phases in the cross section OA.

Figure 2 shows that an increase in α_{l0} (for a fixed ρ_p) does not significantly affect the structure of the gas stream, but it considerably affects the motion of the disperse phase. With increasing α_{l0}, first, the curvature of the particle streamlines increases and the length of the lateral surface ABCD onto which the disperse phase is deposited decreases, and second, the size of the region in which phase transitions occur increases. In Fig. 3 we give distributions of the tangential component of the gas and particle velocities in a channel cross section (x = 3R) for different α_{l0}. One may see from the figure that for all α_{l0} the tangential profile of gas velocity has a characteristic maximum at $r \simeq R/2$, with the gas being swirled as a solid body ($v_1^{\varphi} \propto r$) at $r < R/2$, and in accordance with a potential vortex-free stream ($v_1 \propto \text{const}/r$) at $r > R/2$. A similar effect has been observed in [4] for small r_{20} ($r_{20} \ll 1$). The tangential velocity of the gas decreases with increasing α_{l0} while that of the particles increases. This is because at larger α_{l0}, as moisture is removed from the particle surface, $\beta^{(v)}$ decreases and the force interaction between gas and particle increases, resulting in more intense momentum transfer in the tangential direction. It is shown that with a decrease in the mass concentration of particles at the entrance to the apparatus, the region in which interphase mass transfer occurs decreases, and for $r_{20} \leq 0.1$ its boundary becomes almost stationary. This is because the area of the phase interface at which transfer between gas and moist particles occurs decreases with decreasing r_{20}, leading to an increase in heat flux per unit area of interface. The characteristic time in which the temperature of the moisture in a particle reaches the boiling point therefore decreases with decreasing r_{20}. Starting with some value of r_{20} at which the particles do not affect the motion of the carrier phase, however, the process of heating and evaporation of moisture from the particle surface ceases to depend on the mass content of particles in the disperse stream. It is found that the length of the side surface CD onto which particles are deposited increases with increasing r_{20}. This is because the intensity of the force interaction between gas and particles in the tangential direction increases with increasing r_{20}, resulting in a decrease in the tangential velocities of both the carrier and the disperse phases. The centrifugal force on the particles therefore decreases, which increases the time the particles spend in the central zone of the apparatus. From Fig. 4 it follows that the efficiency of dust removal decreases with increasing r_{20}, as noted in [4] for dry particles. The proposed model thus enables one not only to calculate the

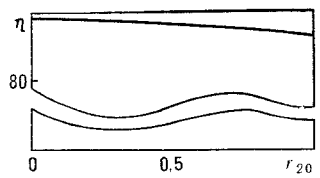

Fig. 4. Efficiency of dust removal as a function of the mass content of particles in the primary stream. η, %.

process of drying and dust removal in apparatus with opposed swirled streams, but also to design the optimum AOSS with allowance for the demands imposed on the dried end product.

NOTATION

r_2) mass concentration of particles; v_i, e_i, E_i, T_i) velocity vector, total and internal energy, and temperature of a phase; p) pressure in the gas; v_i^{φ}) tangential velocity component; n) number of particles per unit volume of the mixture; G_1, G_2) flow rate of the primary and secondary streams; d) particle diameter; R) radius of the apparatus; U_0) characteristic gas velocity; k_{OA}, k_{ED}) twist of the stream in cross sections OA and ED, respectively; U_{ED}) axial velocity of the secondary stream in cross section ED; c_{v1}) specific heat of the gas at constant volume; c_l) specific heat of water; c_p) specific heat of the particle material; γ) adiabatic index of the gas; λ) coefficient of thermal conductivity of the gas; μ_1) coefficient of dynamic viscosity of the gas; σ) coefficient of surface tension of a drop; M) Mach number; $\beta^{(v)}$) inertial parameter of the particles; $\beta^{(\tau)}$) parameter of thermal nonequilibrium of the phases; Re_d, We_d) Reynolds and Weber numbers calculated for the initial gas parameters and particle diameter; j_{0T}) parameter characterizing the intensity of moisture evaporation by the stripping mechanism; j_{0S}) parameter characterizing the intensity of moisture evaporation due to heat uptake; C_a) aerodynamic drag coefficient of a particle; Pr) Prandtl number; Re_{12}, We_{12}) Reynolds and Weber numbers of relative flow over a particle; Nu_{12}) Nusselt number; We_c) critical Weber number; f_{12}, q_{12}) intensities of force interaction and thermal interaction between phases; $j^{(S)}$) intensity of mass transfer due to stripping; $j^{(T)}$) intensity of mass transfer due to evaporation. Indices: i = 1, 2 pertain to the parameters of the gas and particles, respectively; the 0 superscript and subscript pertain to the true and initial state of the medium; the s subscript pertains to the parameters of the medium in the saturated state.

LITERATURE CITED

1. R. I. Nigmatulin, Dynamics of Multiphase Media [in Russian], Vol. 1, Moscow (1987).
2. A. I. Ivandaev, A. G. Kutushev, and R. I. Nigmatulin, Gas Dynamics of Multiphase Media [in Russian], Itogi Nauki Tekh., Mekh. Zhidk. Gaza, 16 (1981).
3. M. M. Gilinskii, A. L. Stasenko, and A. V. Shuinov, Izv. Akad. Nauk SSSR, Mekh. Zhidk. Gaza, No. 3, 36-42 (1987).
4. B. S. Sazhin, Principles of Drying Technology [in Russian], Moscow (1984).
5. V. I. Mushtaev, V. M. Ul'yanov, and A. S. Timonin, Drying Under the Conditions of Pneumatic Transport [in Russian], Moscow (1984).
6. M. V. Lykov, Drying in the Chemical Industry [in Russian], Moscow (1970).
7. I. Kh. Enikeev, O. F. Kuznetsova, V. A. Polyanskii, and É. F. Shurgal'skii, Zh. Vychisl. Mat. Mat. Fiz., 28, No. 1, 9-100 (1988).
8. O. M. Belotserkovskii and Yu. M. Davydov, The Method of Large Particles in Gas Dynamics. Computational Experiment [in Russian], Moscow (1982).